

Influence of L-cysteine engineering on structural and optical properties of nanocrystalline ZnS synthesized by the cost effective chemical co-precipitation method

P. Raja^{a*}, P. Rajkumar^a, P. Jegatheesan^b, A. Sales Amalraj^c, M. Sasikumar^d

^a*P.G & Research Department of Physics, Arignar Anna Government Arts College, Musiri -621211 (Affiliated to Bharathidasan University, Tiruchirappalli, Tamilnadu) India*

^b*Department of Physics, P.S.N.A College of Engineering and Technology, Dindigul-624622, Tamilnadu, India*

^c*PG and Research Department of Physics, Sree Sevugan Annamalai College Devakottai-630 303, Sivagangai (Dt), Tamilnadu, India*

^d*PG and Research Department of Physics, Bishop Heber College (Affiliated to Bharathidasan University), Tiruchirappalli -620 017, India*

Zinc Sulphide (ZnS) nanoparticles were successfully synthesized by the cost effective Chemical co-precipitation method at room temperature. The structural studies were carried out using X-ray diffraction (XRD), Dynamic Light Scattering (DLS) studies were used to analyze particle size, Functional group, optical properties and Morphological study were characterized by FTIR, UV-Vis, PL and Scanning Electron Microscope (SEM). In this work also probe the crystallite development in nanostructure ZnS by X-ray peak broadening analysis. The individual contributions of small crystallite sizes and lattice strain to the peak broadening in Uncapped and L-Cysteine Capped ZnS nanoparticles were analyzed using Modified Williamson-Hall (W-H) analysis. The modified form of W-H plot assuming the uniform deformation model (UDM), uniform stress deformation model (USDM) and uniform deformation energy density model (UDEDM). The root mean square (RMS) lattice strain $\langle \epsilon_{rms} \rangle$ calculated from the interplanar spacing and the strain estimated from USDM and UDEDM are different due to consideration of anisotropic crystal nature.

(Received January 19, 2022; Accepted September 23, 2022)

Keywords: ZnS nanoparticles, Simple Co-precipitation method, X-ray diffraction analysis, Dynamic light scattering, capping agent

1. Introduction

The X – ray diffraction analysis gives the details of measure the average spacing between layers or rows of atoms, determine the orientation of a single crystal or grain. Find the crystal structure of an unknown material and measure the size, shape and internal stress of small crystalline regions. ZnS is a promising semiconductor among II-VI group semiconductors, ZnS has interesting physical, chemical, optical, and electrical properties so that it is using for advanced electronics and optoelectronics devices [1]. Zinc Sulphide exhibits cubic zinc blende and hexagonal wurzite phases and Zinc blende has a stable in room temperature and its significant value of band gap energy (3.63–3.92 eV). The considerable physical properties changes formed duo to their low dimension size range with quantum confinement. The Zinc sulphide nanoparticles have flexible applications in optoelectronics, ultraviolet light-emitting diodes, photo catalysis, flat-panel displays, thin film electroluminescent devices, solar cells, field emitters, injection lasers, spintronics, infrared windows, sensors [2-4]. The applications of ZnS nanoparticles have used as anti microbial agents because of its high surface-to-volume ratio which increases their interaction with micro organisms [5].

* Corresponding author: rajaphysics2007@gmail.com
<https://doi.org/10.15251/CL.2022.199.637>

The ZnS nanoparticle synthesized by various methods are green synthesis [6], simple co-precipitation method [7-10], microwave irradiation method [11], sonochemical method, chemical vapor deposition [12], mechanochemical, solid state reaction, microwave hydrothermal, microwave assisted solvothermal, sol-gel and green synthesis [13]. Among this method, co-precipitation method has enhanced nano property and tunes the size and shape of nanoparticles. Here, the solute is frequently dissolve in the solvent and the reaction can be process in normal temperature and pressure [14]. In order to control size and shape of nano particles capping agents are used and to prevent agglomeration of synthesized nano particle [15].

In this study, a simple and cost effective chemical co-precipitation method was described to prepare pure and L-Cysteine capping agent assisted ZnS nanoparticles. The capping agent effects on structural, optical and morphological studies were investigated in detail.

2. Experimental

2.1. Sample synthesis

Zinc acetate dihydrate [$\text{Zn}(\text{CH}_3\text{COO})_2 \cdot 2\text{H}_2\text{O}$], Sodium sulphide [$\text{Na}_2\text{S} \cdot X \text{H}_2\text{O}$] and L-cysteine extrapure [$\text{C}_3\text{H}_7\text{NO}_2\text{S}$] (L-Cys MW:121.16 g/mol) were used as precursors and distilled water was used as solvent. Synthesis of uncapped ZnS nanostructures, Zinc acetate with distilled water magnetically stirred for 1 hour 30 minutes and Sodium sulphide (Na_2S) with distilled water magnetically stirred for 40 minutes then Na_2S solution taken into separating funnel and mixed into Zinc acetate solution as drop wise. This mixture magnetically stirred for 2 hours to get white precipitation. Distilled water and ethanol are used to purify the obtained samples and it's filtered by whatman filter paper properly to remove impurities of precipitation. Final product was dried in a hot air oven 120°C for 4 hours.

For Synthesis of capped ZnS nanostructures, Zinc acetate with distilled water magnetically stirred for 1 hour 30 minutes and required amount of L-cysteine extra pure with distilled water magnetically stirred for 20 minutes, then zinc acetate solution and L- Cysteine solution mixed and magnetically stirred for 20 minutes and Sodium sulphide (Na_2S) with distilled water magnetically stirred for 40 minutes then Na_2S solution taken into separating funnel and mixed into Zinc acetate and capping agent matrix solution as drop wise. This mixture magnetically stirred for 2 hours to get precipitation. Distilled water and ethanol is used to purify the obtained samples and it's filtered by whatman filter paper properly to remove impurities of precipitation. Final product was dried in a hot air oven 120°C for 4 hours.

2.2. Characterization for uncapped and capped ZnS nanostructures

XRD were used to obtain the textural parameters of the materials, such as size, shape and crystal structure, in order to understand the enhanced properties of capped and Uncapped ZnS nanoparticles. XRD was performed by powder X-ray diffraction (RIGAKU Diffractometer) using $\text{Cu K}\alpha$ radiation (1.5406 \AA) in a $\theta - 2\theta$ configuration and its range from 10° to 70° . Particle size analysis were performed by Dynamic light scattering (DLS) studies using the instrument made by Micromeritics with the model of Nano plus. FTIR spectra were recorded in an FTIR spectrometer (Perkin Elmer make - model of Spectrum Two) in range of 4000cm^{-1} to 400cm^{-1} . UV-Vis measurements were done with UV spectrometer Thermo fisher Evaluation 220 in the wave length range of 190 to 1100 nm. The photoluminescence (PL) with its excitation wavelength analysis was recorded on Varian Cary Eclipse Photo Luminescence spectrophotometer model. Further the morphological properties were carried out by Scanning Electron Microscopy (SEM) analysis using the instrument of Jeol JSM 6390.

3. Result and discussion

3.1. XRD analysis

Infinite of extension is available in perfect crystal in all direction but uniform extension it is not available in the finite size of crystal. Diffraction from the uncapped and L-Cysteine capped ZnS nanoparticle sample occurs, based on Bragg's law $n\lambda = 2d \sin\theta$, where n is an integer, λ is the wavelength of Cu K α radiation, d is the interplanar spacing and θ is the diffraction angle [16]. The XRD peak width shows two main properties there are crystallite size and lattice strain. Imperfection leads to broadening of diffraction peaks. Figure 1 shows the intrinsic Structural behavior of the synthesized uncapped and L-Cysteine capped ZnS nanoparticles used powder X-ray diffraction pattern in the 2θ range of 20° to 70° at room temperature. All the diffraction peaks from uncapped and L-Cysteine capped ZnS nanoparticles could be indexed to Cubic structure of ZnS (JCPDS # 05-0566). No diffraction peaks associated with any other impurities related to the capped agent were observed in all the samples within the detection limit of the XRD. The lattice parameters of the uncapped and L-Cysteine capped ZnS nanoparticles was found that $a=5.368 \text{ \AA}$ and $a=5.385 \text{ \AA}$ respectively. XRD can be utilized to evaluate peak broadening with crystallite size, and lattice strain due to dislocation. The breadth of the Bragg peak is a combination of both instrument and sample dependent effects. To decouple these contributions, it is necessary to collect a diffraction pattern from the line broadening of a standard material such as silicon to determine the instrumental broadening [17]. The observed data

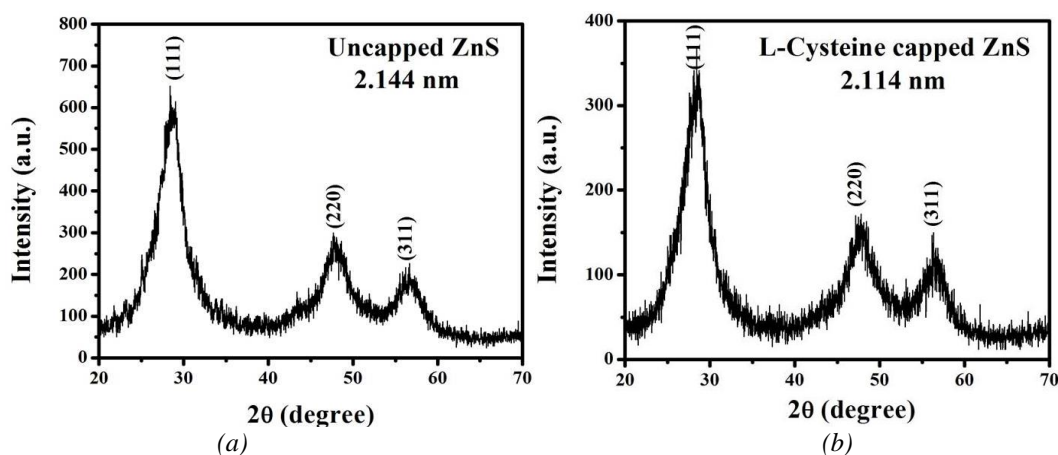


Fig.1.XRD pattern of (a) Uncapped ZnS nanoparticles (b) L-Cysteine Capped ZnS nanoparticles.

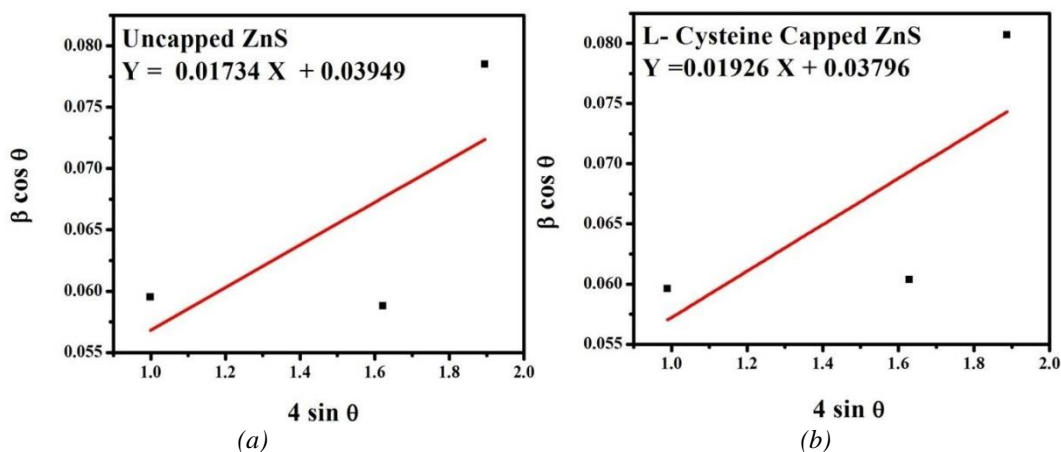


Fig.2. The W-H analysis of (a) Uncapped ZnS nanoparticles (b) L-Cysteine Capped ZnS nanoparticles assuming UDM.

The instrumental corrected broadening β_{hkl} ZnS nanoparticles, corresponding to the diffraction peak of ZnS was estimated by using the relation [18]

$$\beta_{hkl} = [(\beta_{hkl})^2_{\text{measured}} - (\beta^2_{\text{Instrumental}})]^{1/2} \quad (1)$$

Scherer formula [19],

$$D_v = \frac{k\lambda}{\beta \cos \theta} \quad (2)$$

where D_v is the volume weighted crystallite size, k is the shape factor (0.9), λ is the wavelength of Cu $K_{\alpha 1}$ radiation, β_{hkl} is the full width at half maximum in radian, and θ is the angle of reflection (in degrees) was utilized to relate the crystallite size to the peak broadening. The average crystallite size of uncapped and L-Cysteine capped ZnS nanoparticles was obtained from the XRD peaks using Scherer formula (Equ.2) and it was found to be the range of 2 – 3 nm.

Strain induced broadening arising from crystal imperfection and distortion were related by

$$\varepsilon = \frac{\beta}{\tan \theta} \quad (3)$$

From Eqs. (2) and (3) it was clear that the peak width from crystallite size varies as $1/\cos \theta$, whereas strain varies as $\tan \theta$. Williamson and Hall proposed a method of deconvoluting size and strain broadening by looking at the peak width as a function of diffracting angle 2θ and obtained a mathematical expression as

$$\beta_{hkl} = \frac{k\lambda}{D_v \cos \theta} + 4\varepsilon \tan \theta \quad (4)$$

$$\beta_{hkl} \cos \theta = \frac{k\lambda}{D_v} + 4\varepsilon \sin \theta \quad (5)$$

A plot is drawn with $4 \sin \theta$ along the x-axis and $\beta_{hkl} \cos \theta$ along the y-axis for uncapped and capped ZnS nanoparticles. For the entire experiment, the plot is drawn only for the preferred orientation peaks are (1 1 1), (2 2 0) and (3 1 1) of ZnS with the cubic phase. From the linear fit to the data, the crystallite size D_v was extracted from the y-intercept and the strain ε from the slope of the fit. Eq. (5) represents the UDM, where the strain was assumed to be uniform in all crystallographic directions, thus considering the isotropic nature of the crystal, where all the material properties are independent of the direction along which they are measured.

The UDM for uncapped and capped ZnS nanoparticles are shown in Fig. 2. From the plot it the strain associated with uncapped and capped ZnS nanoparticles was 0.01734 and 0.01926 respectively. The generalized Hooke's law states to the strain, keeping only the linear proportionality between the stress and strain, is given by $\sigma = E\varepsilon$. This equation is merely an approximation that is valid for a significantly small strain. Assuming a small strain to be present in the uncapped and capped ZnS nanoparticles, then the ZnS samples obeys Hooke's law to a reasonable approximation. Here, the stress σ is proportional to the strain ε with the constant of proportionality being the modulus of elasticity or Young's modulus, denoted by E . With a further increase in strain the particles deviate from this linear proportionality. As a result, Eq. (5)

$$\beta_{hkl} \cos \theta = \frac{k\lambda}{D_v} + \frac{4 \sin \theta \sigma}{E} \quad (6)$$

Eq. (6) represents USDM, where ε is replaced by σ/E and E_{hkl} is the Young's modulus in the direction perpendicular to the set of crystal lattice planes (hkl). The uniform stress can be calculated from the slope line plotted between $\frac{4 \sin \theta}{E}$ and $\beta_{hkl} \cos \theta$ and the crystallite size D_v from the intercept.

The strain ε can be measured if E_{hkl} of Cubic ZnS nanoparticles are known. For samples with a cubic crystal phase, Young's modulus E_{hkl} is related to their elastic compliances s_{ij} as

$$S_{11} = \frac{C_{11} + C_{12}}{(C_{11} - C_{12})(C_{11} + 2C_{12})} \quad (7)$$

$$S_{12} = \frac{-C_{12}}{(C_{11} - C_{12})(C_{11} + 2C_{12})} \quad (8)$$

$$S_{44} = \frac{1}{C_{44}} \quad (9)$$

Young's modulus of each plane (E_{hkl}) can be expressed for cubic

$$\frac{1}{E_{hkl}} = S_{11} - 2[(S_{11} - S_{12}) \frac{1}{2} S_{44}] \left[\frac{h^2 k^2 + k^2 l^2 + l^2 h^2}{(h^2 + k^2 + l^2)^2} \right] \quad (10)$$

Here C_{11} , C_{12} and C_{44} are the elastic constants of ZnS and their values are 10.79×10^{11} dynes/cm², 7.22×10^{11} dynes/cm², 4.12×10^{11} dynes/cm² [20]. USDM for uncapped and capped ZnS nanoparticles are shown in Figure 3. The USDM values of strains for capped and uncapped ZnS nanoparticles are 0.009148 and 0.010164 respectively. The stress calculated from the slope of the line is slightly greater for the capped ZnS sample than for the Uncapped ZnS nanoparticles.

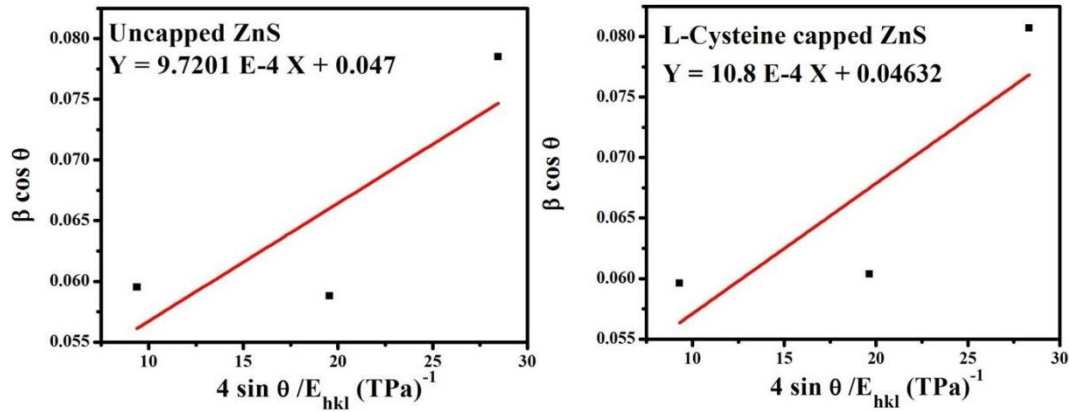


Fig.3. The W-H analysis of (a) Uncapped ZnS nanoparticles (b) L-Cysteine Capped ZnS nanoparticles assuming USDM.

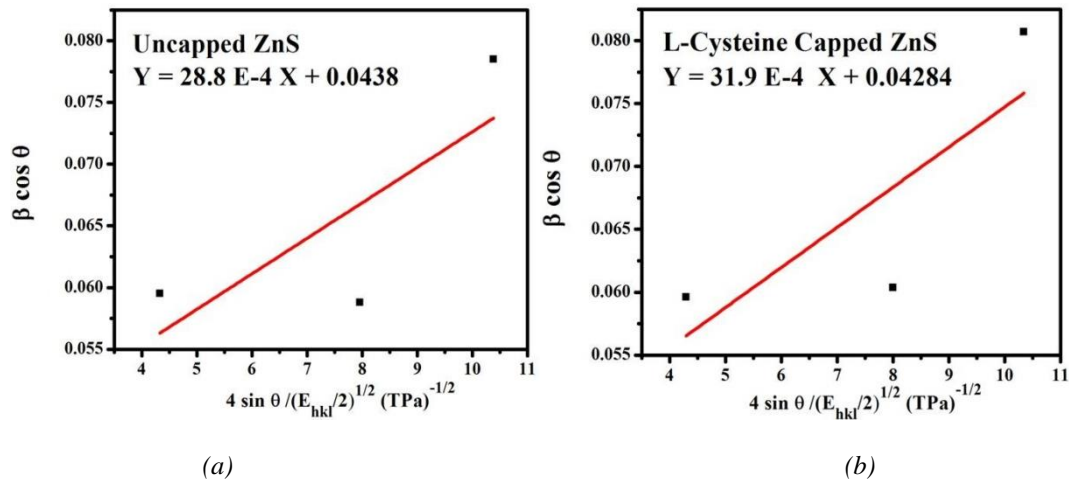


Fig.4. The W-H analysis of (a) Uncapped ZnS nanoparticles (b) L-Cysteine Capped ZnS nanoparticles assuming UDEDM.

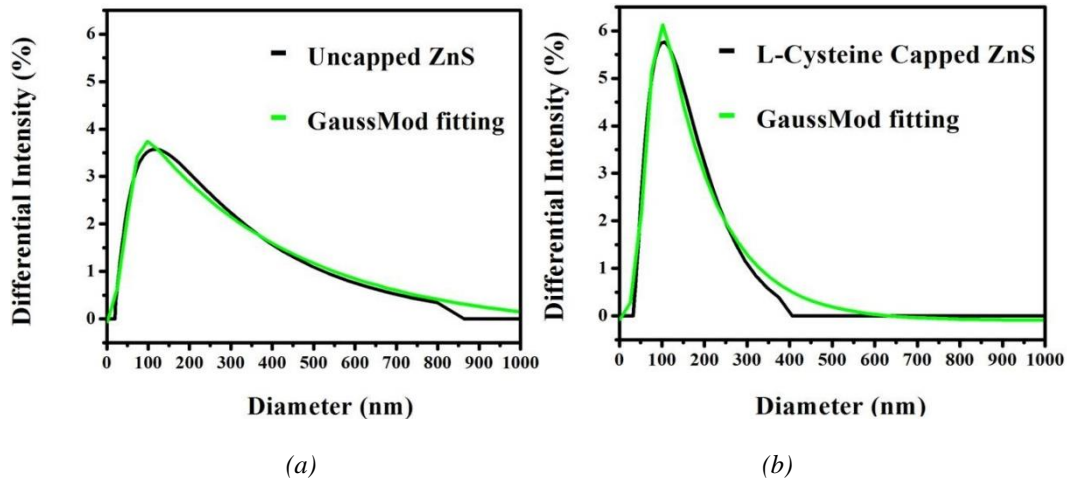


Fig.5. DLS pattern of (a) Uncapped ZnS (b) L-Cysteine capped ZnS.

From Eq. (5) the crystal has been considered as the homogeneous Isotropic nature. But, in many cases, the assumption of homogeneity and isotropy is not fulfilled. Moreover, all the constants of proportionality associated with the stress strain relation are no longer independent when the strain energy density (u) is considered. According to Hooke's law the energy density u (energy per unit volume) as a function of strain ε is $u = \frac{E_{hkl}\varepsilon^2}{2}$. Therefore, Eq. (6) can be modified to the form

$$\beta_{hkl}\cos\theta = \frac{k\lambda}{Dv} + \frac{4\sin\theta(2u)^{1/2}}{(E)^{1/2}} \quad (11)$$

From UDEDM Fig. 4 shows that, a plot is drawn with $\frac{4\sin\theta(2u)^{1/2}}{(E)^{1/2}}$ along the x-axis and $\beta_{hkl}\cos\theta$ along the y-axis for uncapped and capped ZnS nanoparticles. The anisotropic energy density u can be estimated from the slope of the line, and the crystallite size Dv from the intercept, and the strain ε from $\frac{\sigma}{E_{hkl}}$. From the above equations the energy density u and stress σ are related by the equation $u = \frac{\sigma^2}{2E_{hkl}}$. There is a slight difference in the energy density value u obtained in the case of uncapped and capped ZnS nanoparticles. Hence, in anisotropic cubic crystal the strain calculated from the peak position is different from the uniform stress deformation model and uniform deformation energy density model. This result is confirmed from the plot of RMS lattice strain $\langle\varepsilon_{rms}\rangle = (2/\pi)^{1/2} \left(\frac{\Delta d}{d_{0(hkl)}}\right)$ where $\Delta d = d_{hkl} - d_{0(hkl)}$ as a function of interplanar spacing, and the strain estimated from USDM and UDEDM for the uncapped and capped ZnS nanoparticles which are shown in Figs. 3 and 4 respectively. The strain values estimated from the peak position in USDM and UDEDM differ to a greater extent due to the inclusion of anisotropic nature and their values are tabulated in Table 1. Crystalline matter can contain a number of varieties of imperfections, each of which affects the properties of a polycrystalline aggregate.

By W-H models the strain due to the dislocation received at the time of synthesis of ZnS nanoparticles were calculated and tabulated in Table 2. The main contribution is from the chemical reaction and synthesis parameters such as capping agent, pressure and time factor. However, the strain arising from these contributions as calculated from W-H models are very small and have a very minimum effect on peak broadening.

Table 1. Structural analysis of Uncapped and Capped ZnS Nanoparticles.

Sample	2θ degree	Plane (hkl)	d-spacing (Å)	Lattice constant (a) (Å)	Unit cell volume (a) ³ (Å) ³	FWHM (β)	Avg. crystallite Size (D)(nm)	dislocation density (δ= 1/D ²) (lines/m ²)	Average strain (m) (ε _{str} =βcotθ/4)	Stacking fault SF=[(2π ² /45(3tan Θ) ^{1/2})]β
Uncapped ZnS	28.92	(111)	3.08485	5.368	154.68	3.522	2.1448	21.7383x10 ¹⁶	7.753 x 10 ⁻³	0.0284
	48.86	(220)	1.89906			3.688				
	56.57	(311)	1.62559			5.107				
L-Cysteine Capped ZnS	28.65	(111)	3.11330	5.385	156.15	3.526	2.1142	22.3721x10 ¹⁶	7.849 x 10 ⁻³	0.0281
	48.07	(220)	1.89125			3.788				
	56.31	(311)	1.63248			5.246				

Table 2. Young's modulus E_{hkl} stress calculation for uncapped and Capped ZnS nanoparticles.

hkl	E _{hkl} (GPa)		Strain USDM × 10 ⁻³		Strain UEDM × 10 ⁻³		RMS strain <ε _{rms} >=(2/π) ^{1/2} (Δd/d _{0(hkl)}) 10 ⁻³	
	Uncapped	Capped	Uncapped	Capped	Uncapped	Capped	Uncapped	Capped
(111)	106.25	106.25	9.1482	10.1647	1.2494	1.3840	0.0097459	0.002477
(220)	82.9	82.9	11.7249	13.0277	1.6071	1.7738	0.0053998	0.008658
(311)	66.6	66.6	14.5945	16.2162	1.9932	2.2079	0.0036199	0.000254

Table 3. Geometric parameters for uncapped and Capped ZnS nanoparticles.

Samples	Scherer method	W-H Method									DLS
		UDM			USDM			UEDM			
		D _v nm	ε no unit ×10 ⁻⁴	D _v nm	Σ MPa	ε no unit ×10 ⁻⁴	D _v nm	U Kjm ⁻³	σ MPa	ε no unit ×10 ⁻⁴	
Uncapped	2.144	3.511	0.01734	2.950	972	0.009148	3.165	82.94	132.75	0.001249	25.08
Capped	2.114	3.652	0.01926	2.993	1080	0.010164	3.236	101.76	147.05	0.001384	22.61

3.2. Particle Size Analysis Using Dynamic Light Scattering (DLS)

Dynamic light scattering (DLS) also known as Quasi Elastic Light Scattering (QELS) is an ideal technique used to estimate the hydrodynamic particle size of samples like gold nanoparticles, The instrument can measure (Dilution Method) the particle size of samples suspended in liquids in the range of 0.1 nm to 12.3 μm with sample suspension concentrations from 0.00001% to 40%, and a sensitivity for molecular weight to as low as 250 Da. Particle size analysis is used to characterize the size distribution of particles in a given sample. At the same time so many methods

are available to measure particle size and some methods can be used for specific applications and some other methods can be used for wide range of samples. This analysis is based on the concept of light scattered from a solution, undergoing some specific changes in their intensity which is used to as specifically and the size of particles that scatter the light. The average hydrodynamic diameter of the as synthesized ZnS nanoparticles was measured via DLS in ethanol medium [21-25].

Prior the measurement was taken and the sample was first uniformly dispersed in ethanol using ultra sonication for 20 minutes. The obtained dispersed solution was taken in quartz micro cuvette and three measurements were taken from which the average result was recorded. Fig.5. illustrates the average hydrodynamic particle size distribution of the sample with respect to differential Intensity for uncapped ZnS and capped ZnS nanoparticles. The full width half maximum of observed peak was analyzed to expose the particle size using GaussMod fitting calculation. The obtained particle size is to be in the range of uncapped and capped ZnS nanoparticles are 25 nm and 22 nm respectively.

3.3. FTIR Analysis

FTIR Spectrum of ZnS nanoparticles were shown in the Figure 6. In this analysis the IR absorption due to the various vibration modes. When the beam incident on powdered sample, particular frequencies absorbed. At the time interferogram intensities are reduced and proceeding Fourier transform is the sample of infrared absorption spectrum. The IR spectrum showed that the stretching bending corresponding to the characteristic peak at $1500\text{--}1600\text{ cm}^{-1}$ correspond to the carboxyl group (COOH) [26]. C-O around $1350\text{--}1450\text{ cm}^{-1}$ and the C-C linkages around $1000\text{--}1200\text{ cm}^{-1}$ for the capped and uncapped sample. This pointed that the ZnS nanoparticles could be capped with the L-cysteine. The bending vibrations at $3000\text{ to }3500\text{ cm}^{-1}$ band related to O-H stretching vibrations. Zn-S vibrations found in nearer range of 450 cm^{-1} [27].

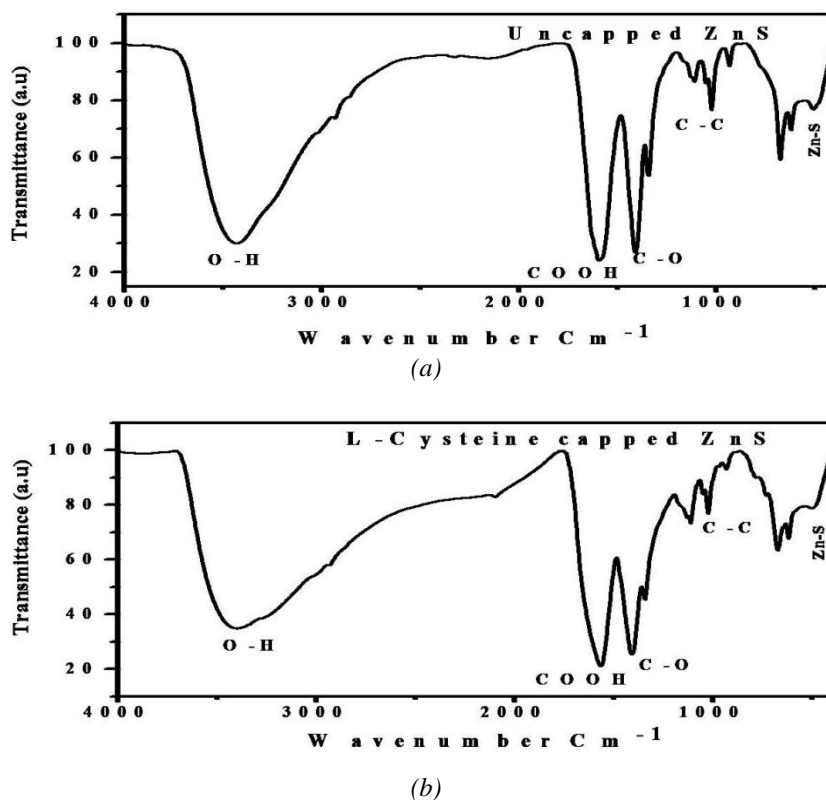


Fig.6. FTIR spectra of (a) Uncapped ZnS Nanoparticles (b) L-Cysteine capped ZnS Nanoparticles.

3.4. Photoluminescence analysis (PL)

Photoluminescence analysis analysis of ZnS nanoparticles was shown in the Figure 7. The semiconductor materials photo generated electrons and holes transfer behavior studied by Photoluminescence characteristics [28]. The broad emission of PL intensity in the range of 400 to 600 nm. From the PL spectra it was observed that Uncapped ZnS and L-Cysteine Capped ZnS nanoparticles showed the emission spectra analyzed and these nanoparticles recorded at room temperature with an excitation wavelength λ_{\max} of 412nm. Broadening of the emission peak is exhibited to both increase the surface states and size distribution owing to increase the surface to volume ratio for nanoparticles [29]. It is considerable thing to mentioning that the presence of dangling bonds and surface state-related imperfections on or near the surface of nano crystals has a valuable effect on their structural and optical properties. In ZnS nanoparticles, significant types of structural and surface defects such as sulfur and zinc vacancies or interstitials result in various emission mechanisms due to the recombination of photo generated electrons and holes [30].

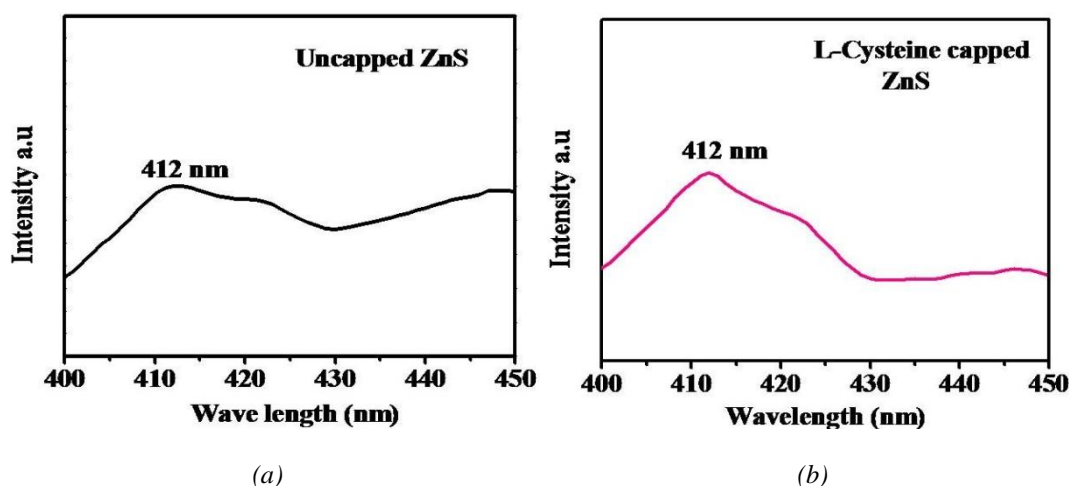


Fig.7. Photoluminescence emission spectra of (a) Uncapped ZnS Nanoparticles (b) L-Cysteine Capped ZnS Nanoparticles.

3.5. UV-Vis Analysis

Ultraviolet (200-400 nm) and Visible (400-800 nm) radiation are found towards the short wavelength, high frequency end of the electromagnetic spectrum. Electronic excitation of electrons between molecular orbital of UV-Vis Absorption spectroscopy measures the percentage of radiation that is absorbed at each wavelength. Typically scanning the wavelength range and recording the absorbance. The ZnS nanoparticles band gap energy can be evaluated from the UV-Vis spectra by using the Tauc relation

$$\alpha h\nu = A (h\nu - E_g)^n \quad (12)$$

where, α is the absorption coefficient, $h\nu$ is the incident photon energy, A is the constant and E_g is the band gap energy of the material. The exponent n depends on the type of transition. The transitions direct and indirect were measured with the n values are $\frac{1}{2}$ and 2 respectively [31]. The band gap energy is estimated by extrapolating the linear portion of the $(\alpha h\nu)^2$ and $(\alpha h\nu)^{1/2}$ vs. $h\nu$ axis to $\alpha = 0$ as shown in Figure 8. The Direct band gap values of uncapped and L-Cysteine capped ZnS nanoparticles are 3.36 eV and 3.45 eV and the indirect band gap values of uncapped and L-Cysteine capped ZnS nanoparticles are 4.43 eV and 4.52 eV. From the analysis L-cysteine amino acid capping played important role for modification in energy gap that is uncapped ZnS has lower band gap compared with L-Cysteine capped ZnS. These results were revealed that particles size decreases band gap increases due to quantum confinement effect.

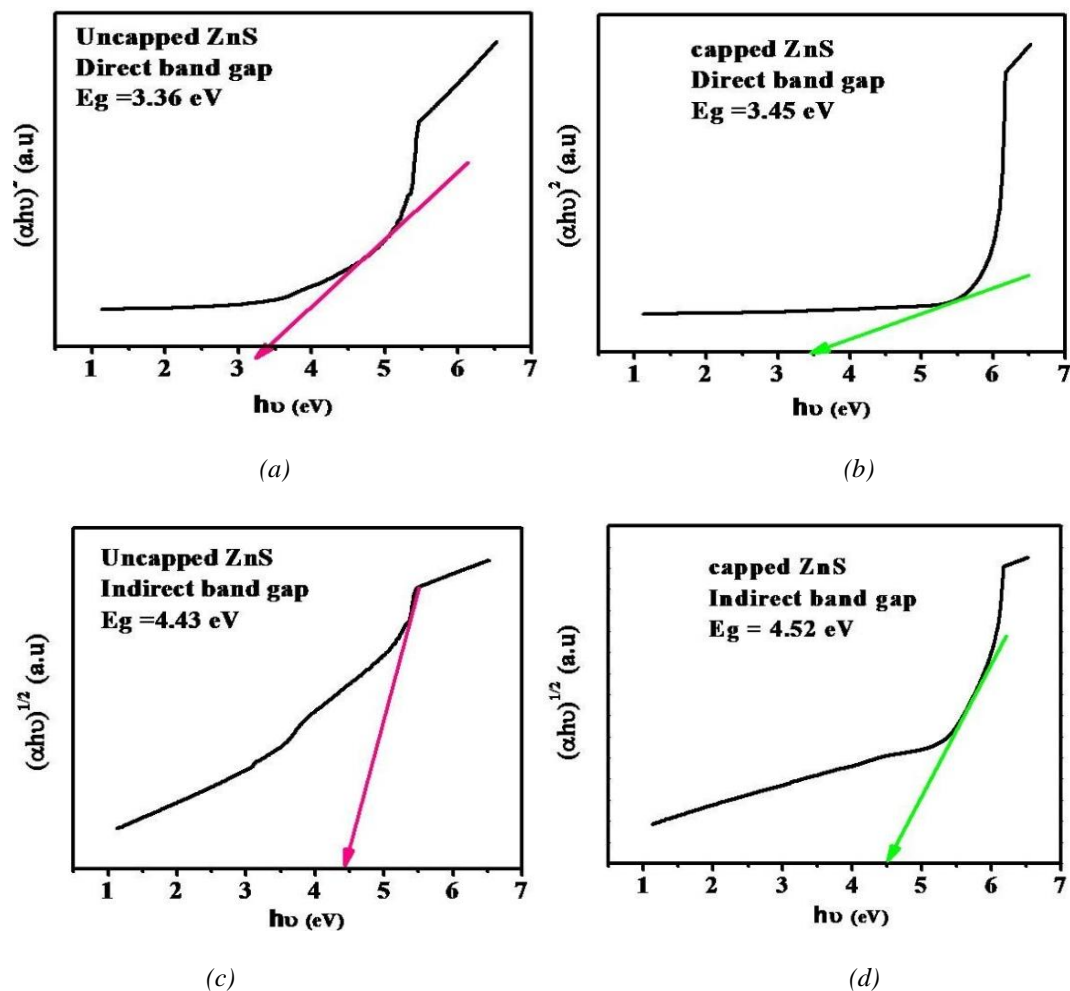


Fig.8. Direct band gap of (a) Uncapped ZnS Nanoparticles (b) L-Cysteine capped ZnS Nanoparticles.

3.6.SEM analysis

The morphological of the Uncapped and L-Cysteine capped ZnS Nanoparticles are investigated by SEM as shown in Figure 9. The ZnS Nanoparticles are the shape with narrow particle size distribution and the nanoparticles formation was varied due to capping agent. From these magnification the considerable agglomeration process were controlled in L-Cysteine amino acid capped Zinc sulphide nanoparticles compared with Uncapped ZnS nanoparticles. The more number of triangle, rhombus, trapezoidal and oval size structures were found in Uncapped sample compared with L-Cysteine amino acid capped ZnS nanoparticles.

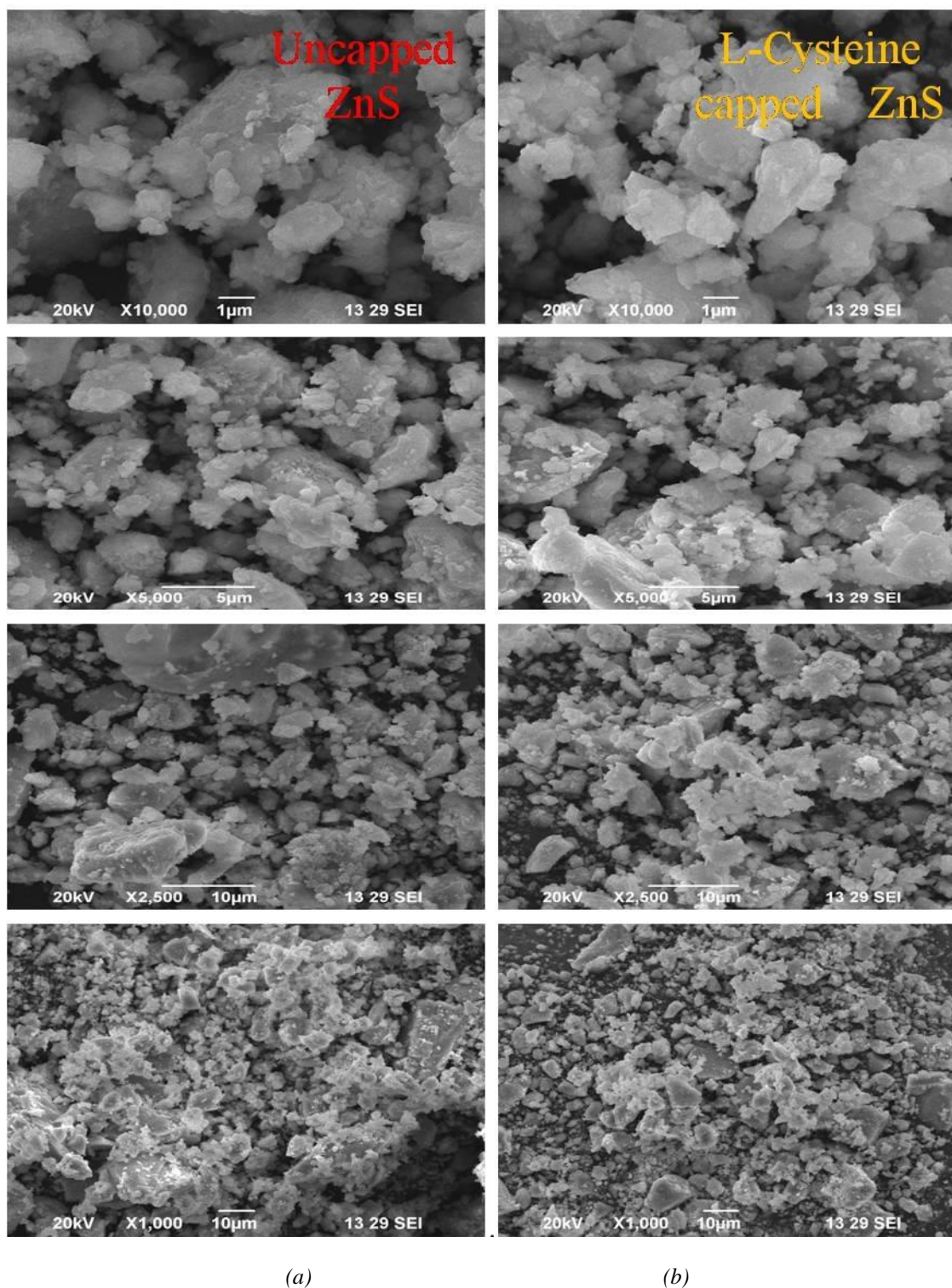


Fig.9. SEM analysis of (a) Uncapped ZnS nanoparticles (b)L-Cysteine capped ZnS Nanoparticles.

4. Conclusion

It is concluded from this work that uncapped and L-Cysteine Capped ZnS nanoparticles were successfully prepared using chemical co-precipitation method, which was further investigated via XRD study for crystallite size analysis along with lattice strain, besides this the

particles size distribution was studied from DLS analysis, which is obtained to be in the range of uncapped and L-Cysteine capped ZnS nanoparticles are 25 nm and 22 nm respectively. The behavior of DLS and Debye Scherer calculation results are similar because their results revealed that size of L-Cysteine capped nanoparticles are smaller than the uncapped nanoparticles.

The average crystallite size and lattice strain has been evaluated through the peak broadening analysis via Uniform Deformation Model (UDM), uniform stress deformation model (USDM) and uniform deformation energy density model (UDEDM) and these from modified form of W-H plot. In the FTIR analysis O-H,C-C,C-O,COOH,Zn-S stretching vibrations were found in both samples. These UV-Vis results were revealed that particles size decreases band gap increases due to quantum confinement effect and the PL excitation wave length are 412 nm .The SEM analysis were revealed that structure variation due to capping effect. The observed data of Structural analysis, Young's modulus E_{hkl} stress calculation and Geometric parameters for uncapped and L-Cysteine Capped ZnS nanoparticles tabulated in table 1, 2 and 3 respectively.

Acknowledgements

The authors are thankful to Advanced Characterization Facility, Centre of Excellence in Advanced Materials & Green Technologies, Amrita Vishwa Vidyapeetham University, Coimbatore-India, for providing XRD analysis. Authors also thankful to Archbishop Casimir Instrumentation Centre (ACIC)

St. Joseph's College (Autonomous), Tiruchirappalli, for providing DLS, UV-Vis, FTIR analysis. SEM facility provided by Karunya University Kovai and the Alagappa University, Karaikudi has provided PL analysis.

References

- [1] S. Kannan, N. P. Subiramaniam, M. Sathishkumar, J. Materials Sci.: Mat. In Elec. 31 (2020) 9846-9859; <https://doi.org/10.1007/s10854-020-03529-x>
- [2] Sathishkumar Mani, Saroja Manickam, Venkatachalam Muthusamy, Rajamanickam Thangaraj, J. Nanostruct. 8(2) (2018) 107-1181
- [3] P. Kannappan, R. Dhanasekaran, IJRTE ISSN: 2277-3878, Volume-7 Issue-4S, 26-28 November (2018)
- [4] Medha Bhushan, Ranjana Jha, Rekha Bhardwaj, J. Phy. and Chem. Solids .135 (2019); <https://doi.org/10.1016/j.jpcs.2019.05.018>
- [5] Thapelo P. Mofokeng, Makwena J. Moloto, Poslet M. Shumbula, Pardon Nyamukamba, Pierre K. Mubiayi, Samkeliso Takaidza, Laurette Marais, Hindawi J. Nanotechnology .(2018); <https://doi.org/10.1155/2018/4902675>
- [6] Subhas Chandra Tudul, Maciej Zubko, Joachim Kusz, Ashis Bhattacharjee, Int. J. Nano Dimens. 11 (2) (2020) 99-111
- [7] Mallappa Mahanthappa, Nagaraju Kottam, Shivaraj Yellappa, Analytical Methods. 10(11) (2018) 1362-1371; <https://doi.org/10.1039/C8AY00007G>
- [8] S. Mohanapriya, M. Vennila, S. Kowsalya, Asian J. Applied Chem. Research .5(1) (2020) 26-33; <https://doi.org/10.9734/ajacr/2020/v5i130125>
- [9] N. V. Desai, I A Shaikh, Adhish V Raval, K G Raval, D V Shah, IOP Conf. Series: Materials Sci. and Engineering 1126 (2021) 012058; <https://doi.org/10.1088/1757-899X/1126/1/012058>
- [10] Md. Sohel Rana, Sujan Kumar Das, Md. Obaidur Rahman, Farid Ahmed, Md. Abul Hossain, Transactions on Elec. and Electronic Materials. (2020); <https://doi.org/10.1007/s42341-020-00265-1>
- [11] B. Lalithadevi, K. Mohan Rao, D. Ramananda, Chem. Physics Letters. 700 (2018) 74-79; <https://doi.org/10.1016/j.cplett.2018.04.010>
- [12] Dasari Ayodhya, Guttena Veerabhadram, Journal of Materiomics. 5 (2019) 446-454;

<https://doi.org/10.1016/j.jmat.2019.02.002>

[13] P. Lokanatha Reddy, Kalim Deshmukh, K. Chidambaram, Mohammad M. Nazeer Ali, Kishor Kumar Sadasivuni, Y. Ravi Kumar, R. Lakshmi pathy, S. K. Khadheer Pasha, J. Materials Sci: Materials in Elec. 30 (2019) 4676-4687;

<https://doi.org/10.1007/s10854-019-00761-y>

[14] K. Vijai Anand, J. Cluster Sci. 32 (2021) 155; <https://doi.org/10.1007/s10876-020-01772-0>

[15] G. Ahmad, A. Batool, Q. Iqbal, A. Iqbal, F. Ali, S. Nawaz, N. A. Shad, M. MSajid and Y. Javed, IOP Conf. Series: Mat. Sci. and Engineering, 863 (2020) 012020;

<https://doi.org/10.1088/1757-899X/863/1/012020>

[16] C. Kittel, Introduction to Solid State Physics, Eighth ed., John Wiley & sons, London, 2005

[17] Rajeswari Yogamalar, Ramasamy Srinivasan, Ajayan Vinu, Katsuhiko Ariga, Arumugam Chandra Bose, Solid State Commun. 149 (2009) 1919;

<https://doi.org/10.1016/j.ssc.2009.07.043>

[18] Debojyoti Nath, Furan Singh, Ratan Das, Mat. Chemistry and Phy. 239 (2020) 122021;

<https://doi.org/10.1016/j.matchemphys.2019.122021>

[19] M. H. Eisa and A. A. Ahmed, Chalcogenide Letters, 18 (12) (2021) 783

[20] Sir C. V. Raman and D. Krishnamurti Proc. Indian Acad. Sci. (1955) A42 111-130

<https://doi.org/10.1007/BF03053497>

[21] Syed Kaabir Ali, Henna Wani, Chandramani Upadhyay, K. S. S. N. Sai Madhur, Imran Khan, Sabia Gul, Nushrat Jahan, Firdaus Ali, Salim Hussain, Kashif Azmi. Indonesian Physical Review. 3(3) (2020) 100-110; <https://doi.org/10.29303/ipr.v3i3.64>

[22] R. Thilagam, A. Gnanamani, Applied Nanoscience 10 (2020) 1879-1892;

<https://doi.org/10.1007/s13204-020-01250-z>

[23] Venu Gopal Bairi, Jin-Hee Lim, Andrew Fong, Sean W. Linder J. Nanoparticle Research. 19

(2017) 256; <https://doi.org/10.1007/s11051-017-3929-0>

[24] Diaa Eldin Fouada, Chunhong Zhanga, Hamdy El-Didamonyc, Liu Yingnana, Tadele Daniel Mekuriaa, Ahmer Hussain Shaha, Results in Phy. 12 (2019) 1253-1261;

<https://doi.org/10.1016/j.rinp.2019.01.005>

[25] Sadhan Kumar Chaudhuri, Lalit Malodia, App. Nanosci. 7 (2017) 501;

<https://doi.org/10.1007/s13204-017-0586-7>

[26] Vivek Pandey, Gajanan Pandey, Vinay Kumar Tripathi, Sapna Yadavd, Mohana Krishna Reddy Mudiam, Luminescence 31 (2016) 341-347;

<https://doi.org/10.1002/bio.2965>

[27] Iftikhar M. Ali, Isam M. Ibrahim, Entissar F. Ahmed, Qayes A. Abbas, Open Journal of Biophysics 6 (2016) 1; <https://doi.org/10.4236/ojbiphy.2016.61001>

[28] K. Ramki, A. Raja Priya, P. Sakthivel, G. Murugadoss, R. Thangamuthu, M. Rajesh Kumar, J. of Mat. Sci: Mat. in Elec.; <https://doi.org/10.1007/s10854-020-03410-x>

[29] K. Vijai Anand, R. Mohan, R. Mohan Kumar, M. Karl Chinnu, R. Jayavel, Inter. J of Nanosci. Vol. 10 3 (2011) 487-493; <https://doi.org/10.1142/S0219581X11008253>

[30] A. P. Alivisatos (1996). J. Phys. Chem. Semiconductor Nanocrystals (1996) 100, 13226-13239; <https://doi.org/10.1021/jp9535506>

[31] S. Prasanth, P. Irshad, D. Rithesh Raj, T. V. Vineesh Kumar, Reji Philip, C. Sudarsanakumar, Journal of Luminescence 166 (2015) 167-175;

<https://doi.org/10.1016/j.jlumin.2015.05.028>